Supplementary Information (SI) for Environmental Science: Nano.

Intercalated MOF Nanocomposites: Robust, Fluorine-free and Waterborne Amphiphobic Coatings

Priya Mandal[1,2], Vikramjeet Singh[1,3], Jianhui Zhang[1,2], Manish K. Tiwari[1,2,3*]

[1]Nanoengineered Systems Laboratory, UCL Mechanical Engineering, University College London, London WC1E 7JE, U.K.

[2]Wellcome/EPSRC Centre for Interventional and Surgical Sciences, University College London, London W1W 7TS, U.K.

[3]Manufacturing Futures Lab, UCL Mechanical Engineering, University College London, London E20 2AE, U.K.

*Corresponding author. Email: m.tiwari@ucl.ac.uk

CONTENTS

Figure S1. PXRD spectra of MOF.

Figure S2. Raman spectra of MOF.

Figure S3. Liquid repellency of WPU-MOF coating at different filler concentrations.

Figure S4: Shear viscosity of WPU-MOF coating immediately after preparation and following one month of storage.

Figure S5. WPU-MOF coating application process on different substrates.

Figure S6. Optimisation of transparency of WPU-MOF coating.

Figure S7. Force-displacement curves for adhesion testing of copper lap joints coated with WPU and WPU-MOF nanocomposite.

Figure S8. SEM image of nanohierarchical MOF embedded in WPU matrix.

Figure S9. Schematic and details of jet impact set-up.

Figure S10. 3D-micropscope image of WPU-MOF coating after repeated jet impacts.

Figure S11. Snapshots of jet impact and 3D-micropscope image of WPU-SiO_2 coating after repeated jet impact test.

Figure S12. Chemical stability of WPU-MOF coating. Variation of θAdv and Δθ in (A) acid (pH~1-2), and (B) alkali (pH~12-13) solution over a period of 24 hours.

Supplementary videos 1-4.

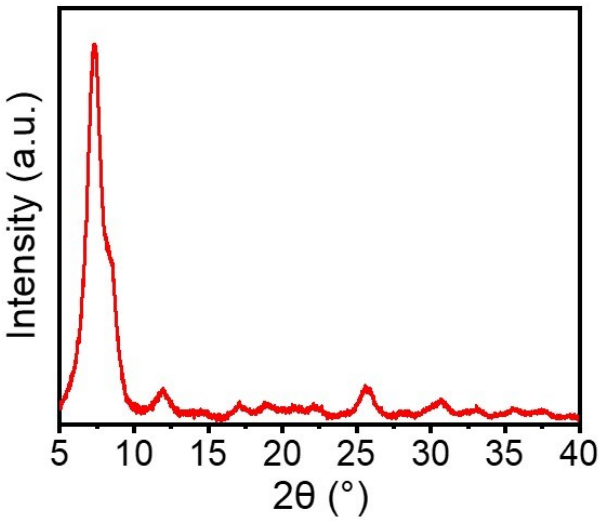

Figure S1. PXRD pattern of MOF.

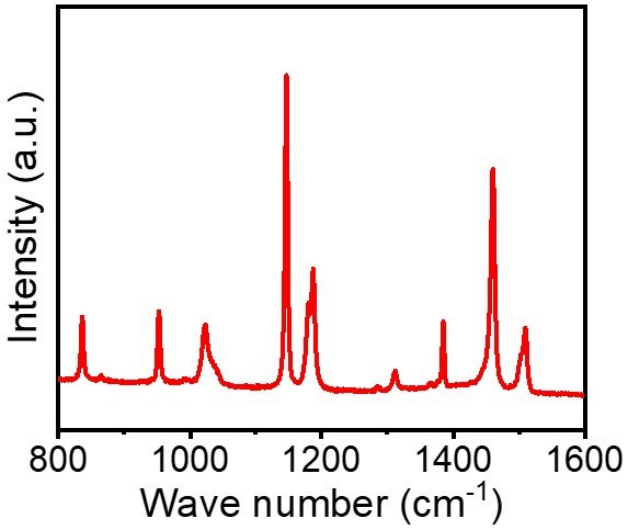

Figure S2. Raman spectra of MOF.

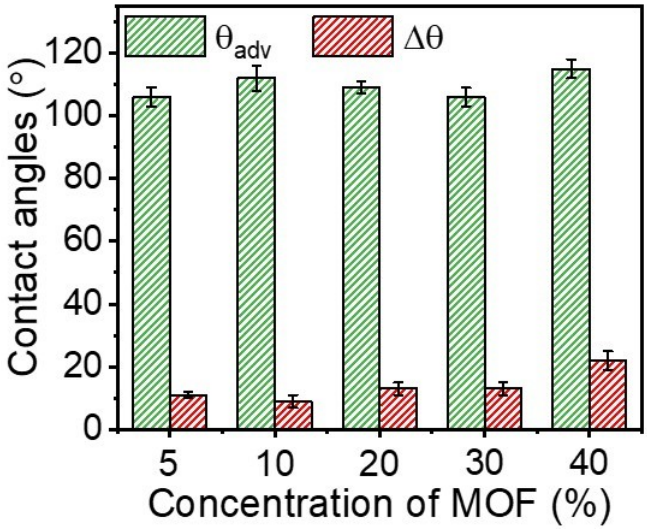

Figure S3. Effect of filler concentration on wettability of the WPU-MOF coating. Error bars represent standard deviation from at least four different measurements at different locations of the coating. WPU-MOF nanocomposites with varying filler concentrations were prepared to determine optimal nanoparticle concentration with best possible liquid repellency.

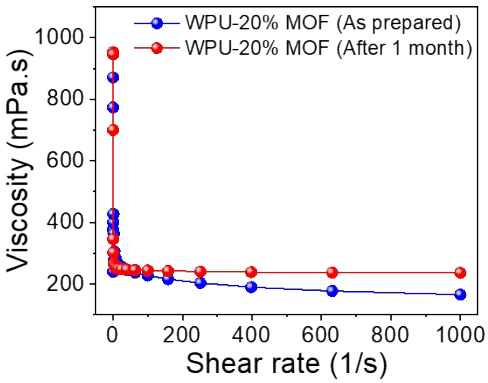

Figure S4. Shear viscosity of WPU-MOF coating immediately after preparation and following one month of storage.

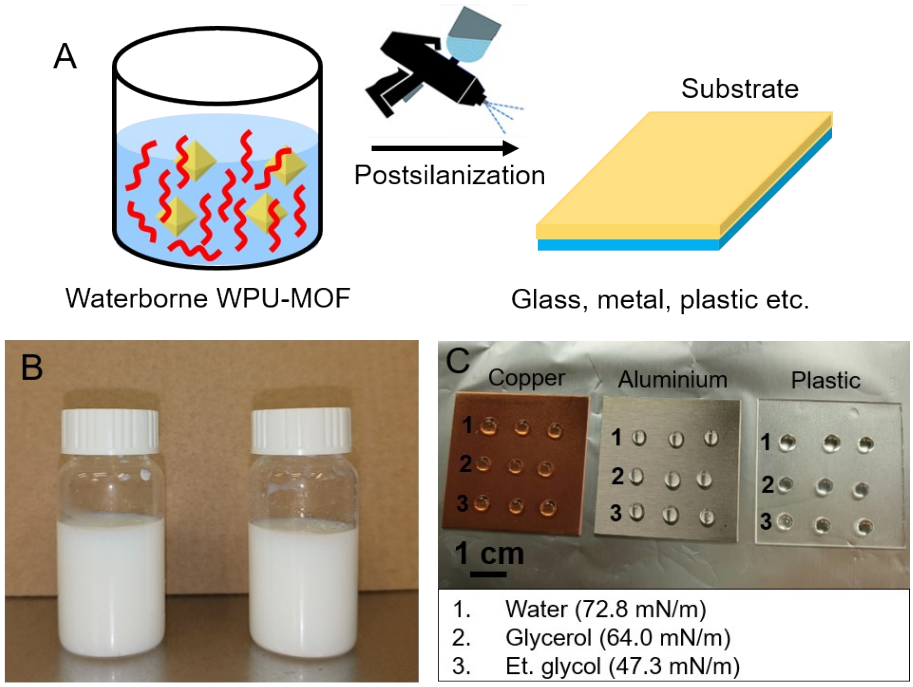

Figure S5. (A) Schematic illustration of WPU-MOF coating via spraying. (B) WPU/MOF/water suspension as prepared (left vial) and stored at room temperature for 1 month (right vial). (C) Optical image of WPU-MOF coating on different substrates: copper (50 mm × 50 mm), aluminium (50 mm × 50 mm), and plastic (50 mm × 50 mm). Liquid droplets of different surface tensions are placed on coated surfaces; 1) Water, 2) Glycerol, and 3) Ethylene glycol.

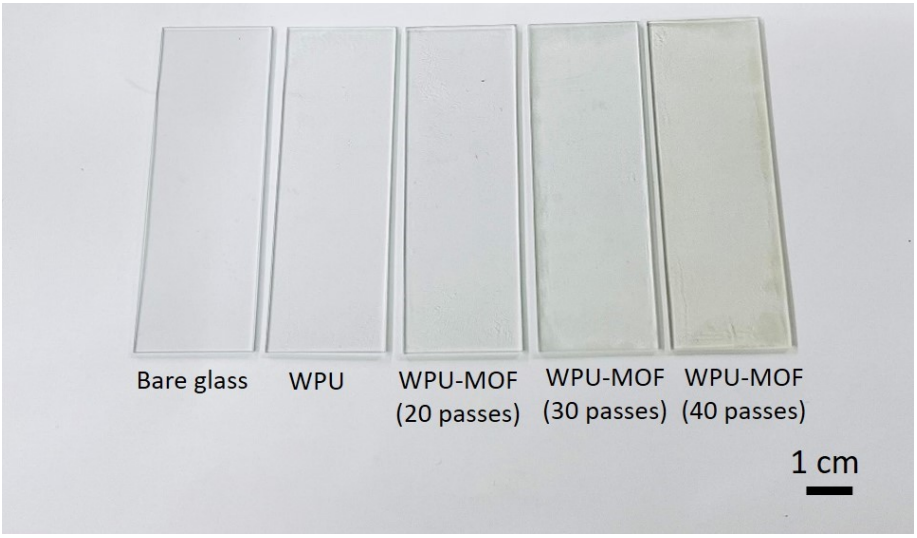

Figure S6. Samples showing effect of spray passes on the transparency.

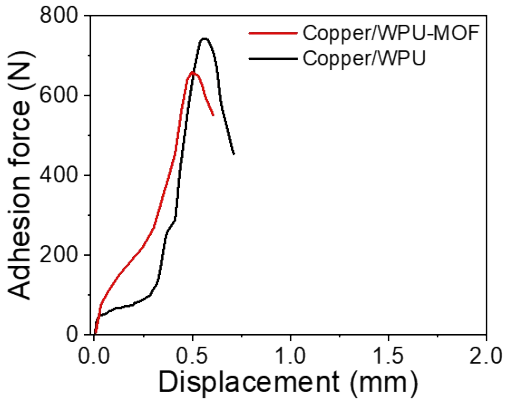

Figure S7. Force-displacement curves for adhesion testing of copper lap joints coated with WPU and WPU-MOF nanocomposite.

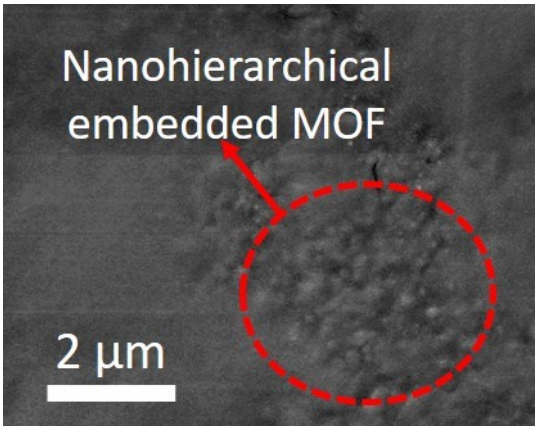

Figure S8. SEM image of nanohierarchical MOF embedded into WPU matrix.

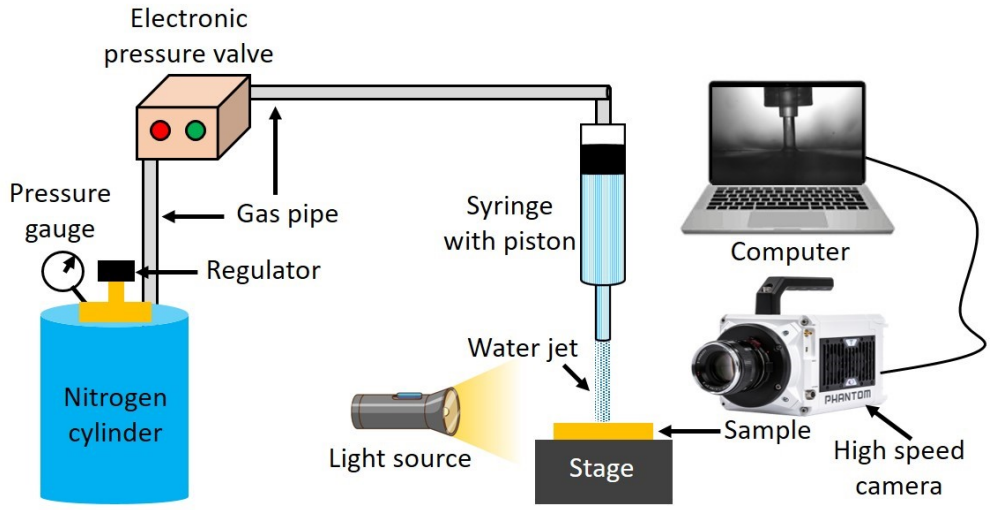

Figure S9. Schematic of water jet impact setup.

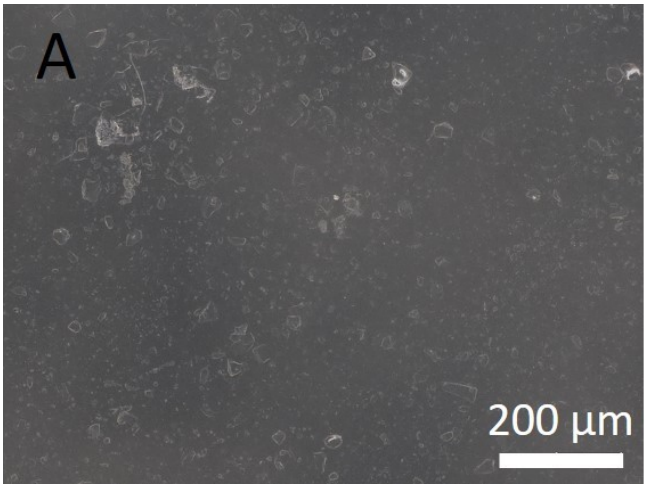

Figure S10. 3D-microscope image of WPU-MOF on glass after repeated jet impacts (3 times) at 35 m/s.

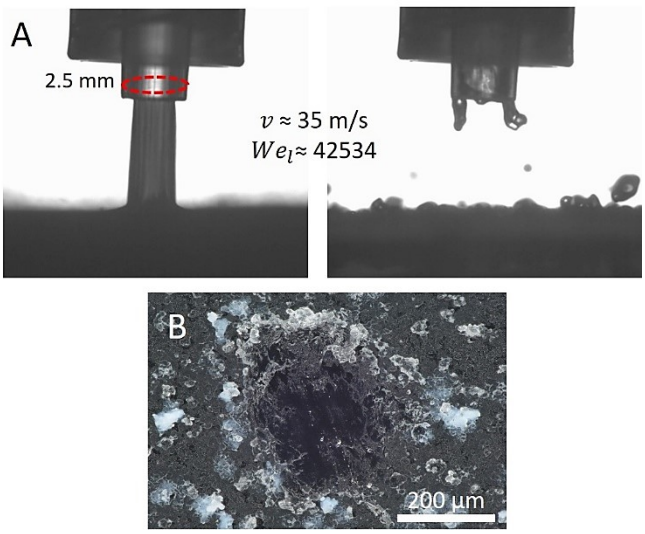

Figure S11. (A) Snapshots of 2.5 mm water jet impacting on WPU-SiO_2 coating vertically with a speed of 35 m/s. (B) 3D-microscope image of WPU-SiO_2 coatings on glass after repeated jet impacts (3 times) at 35 m/s.

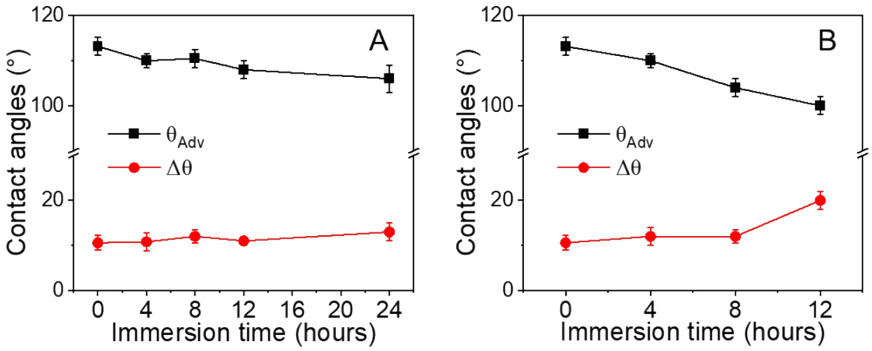

Figure S12. Chemical stability of WPU-MOF coating. Variation of θ_{Adv} and $\Delta\theta$ in (A) acid (pH~1-2), and (B) alkali (pH~12-13) solution over a period of 24 hours.

SUPPLEMENTARY VIDEO CAPTIONS

Supplementary video 1: Free sliding of water (72.8 mN/m) and low surface tension liquid droplets of glycerol (64.0 mN/m), ethylene glycol (47.3 mN/m), and butanol (25.0 mN/m) on WPU-MOF coated glass at 30° tilt angle.

Supplementary video 2: Sliding of water (72.8 mN/m) and butanol (25.0 mN/m) on silanised WPU coating (without MOF nanoparticles) at 30° tilt angle. Traces can be observed on the surface showing poor repellence with butanol.

Supplementary video 3: A water jet with nozzle diameter 2.5 mm impacted on WPU-MOF coating at different velocity (6 m/s, 18 m/s and 35 m/s) recorded by a high-speed camera. The jet impact test was repeated 3 times at the same spot.

Supplementary video 4: Droplet sliding after repeated (3 times) jet impact test. Free sliding of water droplets confirmed lack of pinning and impalement of the coating.